Seminar on Handling and Assembly of Microparts, November 14th, 1994, Vienna, Austria

BSM 3: DESIGN RULES, MODELLING, OPTIMISATION, AND PERFORMANCE OF PRECISION POSITION SYSTEMS FOR SCANNING PROBE, GRIPPING, AND OTHER MEMS APPLICATIONS

Henri Jansen, Rudi Verhagen, and Miko Elwenspoek

MESA Research Institute, University of Twente, P.O. Box 217, 7500 AE Enschede, The Netherlands

Phone: X-31-53-894373; Secr: X-31-53-892751; Fax: X31-53-309547

ABSTRACT

In this paper an xy-stage is fully characterised statically as well as dynamically. It is concluded that the axial stress in the beam is the major non-linear effect. Finite element analysis such as COSMOS is used for the validation of the linear mechanical models. Good conformity between theory and simulation is observed. As a result, mathematical programs such as MATHCAD are now sufficient to predict the mechanical behaviour of structures. This has the advantage that parameters of structures can be altered much easier and faster. After optimisation, xy-stages are developed for their use in scanning probe microscopy. Experiments of devices operated in open air and even under fluid show good agreement with theories.

1. INTRODUCTION

In fine mechanics, it is often necessary to manipulate devices quickly and accurately into a new position, sometimes even along a well defined trajectory and at the same time maintaining a prescribed position. Such devices are referred to as precision position systems. A good precision system should be strong, light, stiff, cheap, accurate, and free of hysteresis, creep, and clearance.

Precise positioning in the xy-plane is possible with the xy-stages presented in this paper. Figure 1 shows one of the fabricated xy-stages. The functional components of the stage are the suspension (spring), which gives a mechanical guidance for the actuator movement, and the electrostatic comb actuator, where the pulling force for the actuation is created. The centre of the stage is moved to any position in the xy-plane by energising two of the four comb-drives.

Two xy-stage flexure designs are presented. Special attention has been paid to the optimisation of the flexure design because this is the key to a properly functioning device. One of these flexures is capable of creating only very small deflections because axial stresses in these beams are maximised resulting in strongly non-linear behaviour (fig.1). In contrast, a second design is suitable for large deflections because axial stresses in the beams are absent, exhibits good decoupling between the x- and y-direction and results in a stable device. Depending on the customer, the design of a MEMS device can be optimised for a certain goal.

In order to design xy-stages that meet certain specifications, the behaviour of the stages has been fully characterised. The static and dynamic behaviour of the flexures have been modelled using the theory of linear elasticity and Raleigh's method (spring rates, fundamental resonance frequency, quality- or Q-factor, and response time). Validation of the mechanical models has been done with linear finite element simulation.

For large displacements the mechanical behaviour may suffer from certain non-linear effects. In general, the spring rates in the desired direction of motion increase as a result of these effects. This is disadvantageous because low driving voltages are desirable. A summary of work on the non-linear behaviour of a double-sided clamped beam is presented.

Preceding chapters have been purely concerned with mechanics, the actuators used to generate the mechanical force have been left out of consideration. To give a complete description of xy-stages, this chapter establishes the necessary models about the transduction between the electric and mechanic domain. Secondly, criteria regarding the stability of comb-drives are described.

Xy-stages are developed with the recently developed black silicon method (BSM) at the University of Twente which is based on the reactive ion etching (RIE) of silicon. With this method, flexures are made of single-crystal silicon (SCS). This is very advantageous because SCS has high intrinsic Q-factors, very low fatigue, low hysteresis and no built-in stress.

Measurements on the xy-stages manufactured with this process will be presented.

Before this paper is proceeded a word of caution is given: The constructions found in this paper are not optimised with respect to their degree of statical indeterminacy. In simplified words, the construction is hold by too many beams. Preferably, this degree should be zero i.e. a statically determinate construction. The intermezzo after this paper will deal with this problem more extensively.

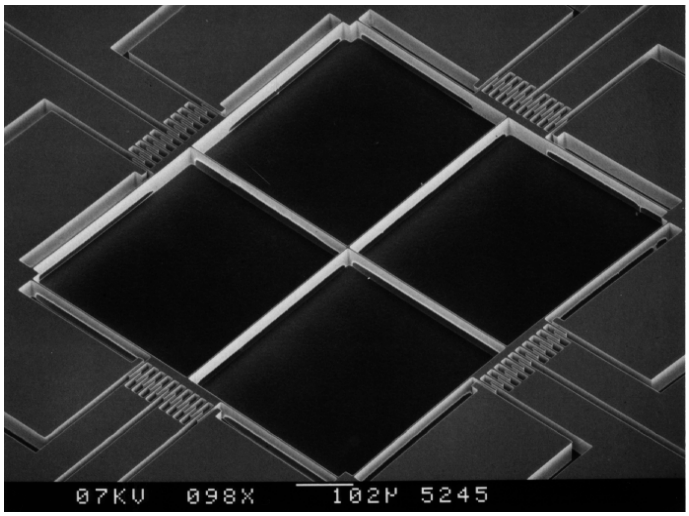

Fig.1: SEM of a comb-driven xy-stage

2. STATIC MODELLING OF SPRINGS

Springs are the basic structures xy-stages are constructed with. First of all, research has to be done to decide which spring design is most suitable for a given application. Secondly, relevant properties of springs have to be modelled. Seven possibly useful flexure suspensions are presented in fig.2, with desired direction of motion, x, and undesired direction of motion, y. To repress the motion in the undesired direction of motion, k_y has to be much larger than k_x. Secondly, small spring rates in the desired direction of motion are demanded to be able to use low driving voltages.

It is assumed that the relatively thick sections of the flexures (represented in grey) are completely rigid. For k_x, this assumption is very accurate due to the fact that k_x is proportional to h^3/L^3 (with: h=height of beam and L=length of beam). For the mechanical spring rate in the y-direction, this assumption is far less accurate. This is caused by the fact that k_y is proportional to h/L.

The spring rates for spring 2 to 7 have been derived in the following manner. The mechanical spring rates of a clamped beam (spring 1) in both directions can be derived rather straightforward using standard linear elastic theories [1,2]. The spring rates of spring 2 to 7 in proportion to the spring rates of spring 1 can be calculated by simply using ones common sense.

Spring 1: The first step is to obtain equations for a clamped beam. The equations can be derived from the simple beam theory by using the geometrical symmetry of the structure and the boundary conditions at the ends of the beam. The deflection at any position, y, along the beam due to a force F_x has to be known for the dynamic modelling of springs. The deflection x(y) due to F_x of the left half of a clamped beam is represented below:

$$x(y) = F_x y^2 (3L - 4y) \Big/ 4Ebh^3 \qquad [1]$$

and the resulting slope and deflections in the middle of the clamped beam are:

$$\varphi = 3M_z L \Big/ 4Ebh^3 \qquad [2]$$

$$x = F_x L^3 \Big/ 16Ebh^3 \Rightarrow k_{x1} = 16Ebh^3 \Big/ L^3$$
$$y = F_y L \Big/ 4Ebh \Rightarrow k_{y1} = 4Ebh \Big/ L \qquad [3]$$

with: b=width of beam, h=height of beam, L=length of beam, E=modulus of elasticity or Young's modulus, F_x=force in the direction of the X-axis, F_y=force in the direction of the Y-axis, M_z=moment along the Z-axis, φ=angle of rotation around the Z-axis.

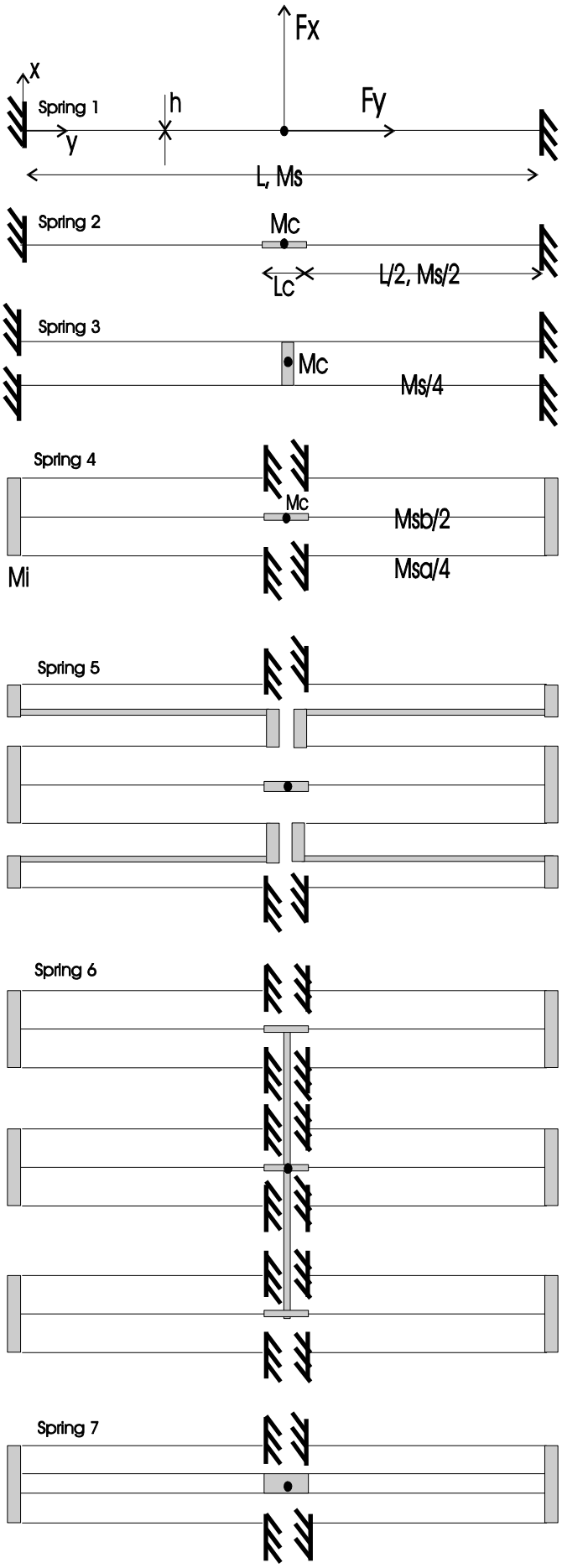

Fig.2: Summary of spring configurations.

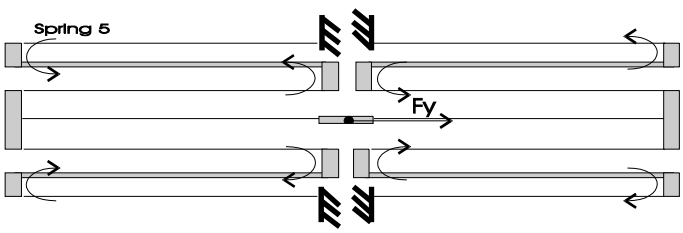

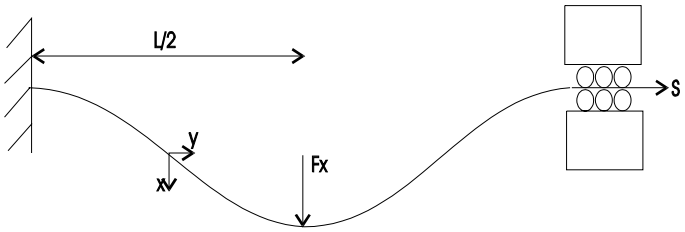

Fig.3 left: Undesired behaviour of spring 5 in the y-direction of motion.
Fig.4 right: One-sided clamped beam. Only the slope and x-translation of the other end of the beam is restricted.

Spring 2: Another basic spring configuration can be compared with a normal clamped beam. the difference however is an extra thick beam section in the middle of the clamped beam. The spring constants in the x-and y-direction are assumed to be equal to a normal clamped beam because it is assumed that the thick beam section is completely rigid. Rotation as a result of an applied moment around the Z-axis is fundamentally different from the rotation of a clamped beam. It can be found, compared to the uniform clamped beam, that the rotation is decreased with the factor: $L^2/(L^2+3LL_c+3L_c^2)$ with L_c=length of thick beam section and L is total length of thin beam section.

Spring 3: This spring is build up with two clamped beams placed in parallel. In other words, it is two times less flexible and therefore $k_{x3}=2.k_{x1}$ and $k_{y3}=2.k_{y1}$.

Spring 4: First of all it should be stated that the slope of the beams is zero at places where the beams are clamped, at the connection points with the thick beam sections and due to symmetry, in the middle of the long thin beam. Therefore, the long thin beam has the same boundary conditions as the clamped beam. The deflection of this section in the x-direction, x_1, is therefore F_x/k_{x1}. The two flexural sections consisting of two short beams, will be deflected half this distance. As a result $k_{x4}=2/3.k_{x1}$. For the y-direction, k_y of each short beam section is $2.k_{y1}$. This spring consists of two pairs of short beams having a spring rate of $4.k_{y1}$. The total elongation in the y-direction therefore becomes $1/4.y_1+y_1+1/4.y_1=3/2.y_1$. As a result $k_{y4}= 2/3.k_{y1}$.

Spring 5: This spring can be more or less compared with spring 4. The only difference is the fact that one rigid and one flexural beam section are added. The total deflection becomes $x_1+2.x_1/2=2.x_1$. As a result $k_{x5}=1/2.k_{x1}$. The mechanical spring rate in the y-direction is much lower as would be expected from simple elasticity theory. This phenomenon is due to undesired rotations and is illustrated in fig.3. As a result the selectivity, which is the ratio of k_y to k_x is decreased rapidly and therefore spring 5 is useless for xy-stages.

Spring 6: Three spring 4 flexures are placed in a parallel connection and therefore it can be stated that $k_{x6}=3.k_{x4}=2.k_{x1}$ and $k_{y6}=3.k_{y4}= 2.k_{y1}$.

Spring 7: This spring can be compared with spring 4. The difference however is that the two long thin beams are twice as rigid as the single long thin beam of spring 4. The total deflection becomes $1/2.x_1+1/2.x_1=x_1$ and $1/4.y_1+1/2.y_1+1/4.y_1=y_1$. As a result $k_{x7}=k_{x1}$ and $k_{y7}=k_{y1}$.

To suppress the motion in the undesired direction of motion, k_y has to be much larger than k_x. In other words, the selectivity, S, has to be as large as possible. Except for spring 5, S is expressed by the following equation: $S=k_y/k_x=(L/h)^2/4$. Which spring configuration is most suitable depends on the application. Examples of possibly desired spring properties are:

1) Small spring rate in the desired direction of motion: Especially spring 5 and, to a smaller extend spring 4, meet this demand.
2) Large spring rate in the undesired direction of motion: Spring 5 has a reduced k_y due to the rotation of certain parts and is therefore unsuitable for xy-stage applications.
3) Suitable for large deflections in the desired direction of motion: Spring 1, 2 and 3 are not suitable for large deflections because of the clamping of the beams. As a result, elongation of the beams is limited due to large axial stresses. The axial stresses can be minimised by using spring 7. The interconnecting thick beam section at the ends can move freely in the y-direction. This is due to the fact that all thin beams have identical shapes and therefore wish to move inwards in the same amount. Spring 4 can also be modified in order to reach zero axial stresses. Adjusting the height of its middle beam with a factor $2^{1/3}$ also gives beams with identical shapes and identical deflections resulting in zero axial stresses. However, from a technological viewpoint such a solution is less attractive because it is "easier" to fabricate beams with *exactly* the same shape than to create a beam *exactly* two times bigger than a reference beam.
4) Small comb rotation: Due to the fact that several beams are spaced apart, spring 3, 6 and 7 are more or less rotation-free.

On the whole it can be concluded that spring 7 is most suitable because the spring rate will be constant for relatively large deflections because axial stresses are avoided. Furthermore, rotation of the comb is avoided which increases the stability.

3. NON-LINEAR THEORY

Up to this point, mechanical models based on the theory of linear elasticity were derived. In realistic situations however, geometrical non-linear effects may severely influence the mechanical behaviour of the flexure. Especially double-sided clamped beams suffer from these effects. Study on the non-linear effects in such flexures has been done [3].

The derivation of the non-linear deflection curve has been simplified by using a few assumptions. It has been concluded that these simplifications have a very small influence compared to the influence of axial stress in the beam. The following effects have been neglected:

1) Change in cross section area due to elongation of the beam.
2) Warping of the cross sections of a beam due to anti-clastic deformation.

Moreover, the deflection curve is simplified by stating that the slope of the beam is much smaller than unity.

Starting point for the solution of the non-linear behaviour is the differential equation for a clamped beam including axial stress:

$$EIx(y)^{(4)} - S(x)x(y)^{(2)} = 0 \qquad [4]$$

In this equation EI represents the flexural rigidity, S the axial stress, y is the location on the beam, and x the deflection of the beam. Solving this equation yields (for -L/4<y<L/4):

$$x(y) = \frac{F_x}{2S}\left(y - \frac{\sinh(qy)}{q \cdot \cosh(qL/4)}\right) \qquad [5]$$

Where F_x is the external force in the x-direction and $q=\sqrt{[S/EI]}$. In fig.4, the problem is illustrated. The double-sided clamped beam is replaced with a one-sided clamped beam. The slope of the other end of the beam is kept horizontal by the wheels. The axial force, S, can be controlled independently. The calculation starts with the linear equation of the deflection curve, in other words the situation where S equals zero. With this linear equation, the elongation of the beam is determined. The algebraic solution of the elongation is approximated with a Taylor polynomial because otherwise the analytical solution becomes too complicated. The next step is to determine the reaction force, S, needed to pull the end to its initial position. It should be noted that S is not accurate because the linear deflection curve was used. To determine the correct value for S, we have to iterate the deflection until it converges to a certain value. After iteration, the non-linear deflection curve (up to the 3rd order) is found:

$$x(y) = \frac{Fy}{2Eb(2h)^3}(3L^2 - 16y^2) - \frac{9F^3L^4y}{200E^3b^3(2h)^{11}}(5L^2 - 16y^2)^2 \qquad [6]$$

The final result is the non-linear deflection at the middle of the clamped beam (y=L/4):

$$x_{non\text{-}linear} = x_{linear}(1 - 2(3FL^3/40Ebh^4)^2) \qquad [7]$$

From this equation it can be calculated that the non-linearity becomes important (>10% of the linear deflection) when the deflection of the beam exceeds only h/6!

4. DYNAMIC MODELLING OF SPRINGS

The complete solution of the problem of free vibration would require the determination of all natural frequencies and the mode shape associated with each. The mode shape (χ) describes the displacement at any point of the spring, in relation to the maximum deflection of the spring. In practice, it often is necessary to know only a few of the natural frequencies, and sometimes only one. For xy-stages only the lowest frequency is of importance. The exact mode shape is of secondary importance. This is fortunate since Raleigh's method is based on assuming a mode shape.

Raleigh's method: It is often very simple and direct to use energy methods to solve vibration problems. Energy methods, such as Raleigh's method, involve an energy balance using scalars rather than a force balance with vectors [4].

The fundamental frequencies of spring 1, 2, 3, 4 and 7 will be given in this section. It is assumed that the oscillation of the flexure can be expressed as a simple harmonic motion of the generalised co-ordinate, x. A very reasonable estimation for the fundamental mode shape is the deflection due to a static load F_x. This estimation will be used to determine all resonance frequencies.

Spring 1: Equating the maximum kinetic energy to the maximum potential energy and solving for the frequency gives the following result:

$$\omega_{r1} = \sqrt{k_{x1}/13m_s/35} = \sqrt{16Ebh^3/13m_sL^3/35} \qquad [8]$$

with m_s (s=spring) the mass of the thin beam. It can be seen that the effective mass of the flexure is 13/35 th of its actual mass.

Spring 2: Compared to spring 1, the only difference is the thick beam section with mass m_c (c=comb). Therefore, the resonance frequency becomes:
$\omega_{r2}=\sqrt{[16Ebh^3/(m_c+13m_s/35)L^3]}$.

Spring 3: This flexure can more or less be compared with spring 2. The only difference compared to spring 2 is the fact that the equation to describe k_x will be changed, because this flexure is half as flexible (using the same dimensions). Of course, the masses have to be altered in order to describe the current configuration. The resonance frequency is:
$\omega_{r3}=\sqrt{[32Ebh^3/(m_c+13m_s/35)L^3]}$.

Spring 4: First of all, the total kinetic energy has to be determined. For this purpose, the flexure is divided into sections of which the kinetic energy is evaluated separately. To be able to evaluate the kinetic energy, the mode shape has to be known. It is expected that the ratio between the maximum deflection of the thick interconnecting beams ($x_{i,max}$) and the thick comb beams ($x_{c,max}$) depends on the ratio of m_i, m_c, m_{sa}, m_{sb}. For instance for large m_i/m_c-ratios, $x_{i,max}$ is more or less equal to $x_{c,max}$. The ratio of the latter maximum deflections will be varied in order to obtain the ratio at which the resonance frequency is lowest: $x_{i,max}=x_{c,max}/n$. Equating ΔT_{max} and ΔV_{max} gives the following resonance frequency as a function of n:

$$\omega_{r4} = \sqrt{\frac{16Ebh^3(n^2-2n+3)}{(m_i + \frac{13}{35}m_{sa} + (\frac{13}{35}n^2 + \frac{9}{35}n + \frac{13}{35})m_{sb} + n^2m_c)L^3}} \qquad [9]$$

The mode shape resulting in the lowest resonance frequency is the actual mode shape. Therefore, n has to be solved by minimisation of $\omega_{r4}(n)$. This is done by taking the partial derivative of ω_{r4}^2 to n, equating to zero and solving for n.

Spring 7: The calculation method for the resonance frequency of spring 7 is almost identical to the procedure for spring 4. The only difference between the two structures is the fact that this time the middle thin beam section consists of two beams instead of one. The resonance frequency is found by replacing the factor (n^2-2n+3) by 2(n^2-2n+2) in the formula of spring 4.

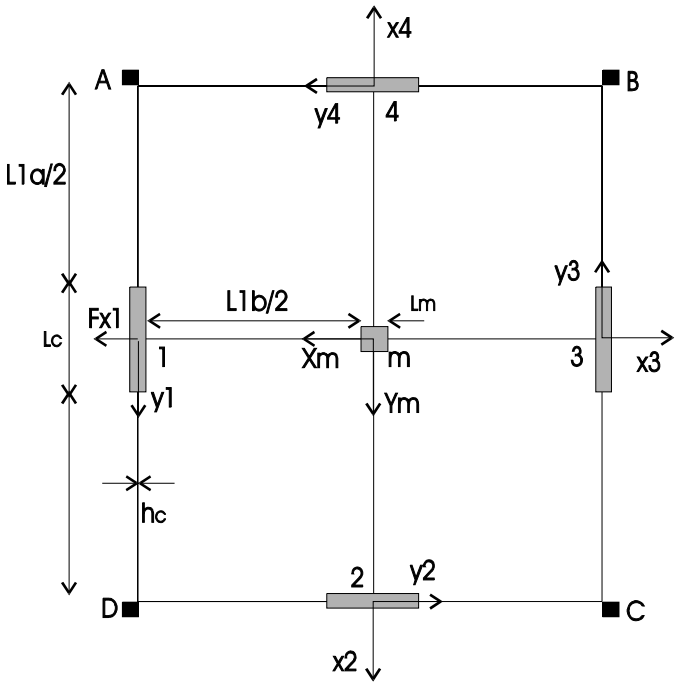

Fig.5: Xy-stage 1 constructed with clamped beams. The beams are fixed to the substrate at points A, B, C, and D.

5. STATIC MODELLING OF XY-STAGES

This chapter deals with modelling of so-called comb-driven micromechanical xy-stages. In fig.1 a SEM picture of an xy-stage is given. The structure consists of four electrostatic combs suspended by a mechanical structure. When a driving voltage is applied to the fixed electrodes, the comb generates a pulling force. The mechanical structure accomplishes two tasks. First of all, it guides the actuator force to the centre of the stage. Secondly, it prevents the moving electrode to touch the stationary electrode which would cause the comb actuator to stop operating. By selectively actuating certain combs, the centre of the xy-stage can, within a certain range, be positioned in the xy-plane. It is desirable that such devices have the following mechanical and electrical properties:

1) Good uncoupling of the in-plane translational degrees-of-freedom (DOFs) x and y and little hysteresis of the mechanical structure. If these conditions are satisfied, precise positioning in the xy-plane is possible.
2) Suppression of undesired translations and rotations of the moving electrodes. In other words, stability of the comb actuators should be guaranteed.
3) Suitability of the mechanical structure for large deflections and low driving voltages to reach those large deflections.
4) Low friction, fatigue and wear. Furthermore, it is convenient if the structures is robust with regards to external disturbances.

Two xy-stage designs are presented in this chapter. Both designs can be treated theoretically in the same manner and with the help of the models of the springs presented in the previous chapters. For every device, the qualitative behaviour can be described followed by the quantitative modelling of the interesting co-ordinates separately. Finally, the total relationship between all actuator forces and all relevant co-ordinates can be given in the form of a matrix equation.

Xy-stage 1: The first xy-stage configuration is constructed with clamped beams and is frequently discussed in literature (fig.1 and fig.5). Despite its advantageous simplicity, it is expected that this design has some major disadvantages, namely:

1) Xy-stage 1 is constructed with clamped beams which have the disadvantage that they are not suitable for large deflections. This results from the fact that forces resulting from the elongation of the beam, will work against further deflection of the clamped beam. This non-linear effect will be dominant even for relatively small deflections.
2) The comb-fingers of comb 2 and 4 will start to rotate due to a driving force F_{x1}. Especially for long comb-fingers rotation can result in short-circuits between the free and fixed electrodes. When this occurs, the comb actuators will stop operating.
3) The moving electrodes of comb 2 and 4 will move inwards when for instance a force F_{x1} is applied. This is due to the fact that elongating a beam requires much more effort than deflecting a clamped beam in the direction normal to the beam. Motion in the xy-plane is poorly uncoupled as a result of this effect.

The spring constants of clamped beams have already been derived. The two beams placed crosswise in the middle of the device however, have different boundary conditions than clamped beams and therefore different spring rates. As a result, the spring rates of this structure have to be established first to be able to determinate the spring constants of the entire xy-stage structure.

The next step is to determine the displacement of mass m in the x_m-direction theoretically. Having established the spring rates of all substructures, the equivalent spring constant of xy-stage 1 can be found. This is done by noticing that some flexures are connected in a series and others in parallel connection. The described models are capable of predicting the translations and rotations due to one actuator force. When a combination of forces is applied to the structure, the situation becomes more complex. Fortunately, superposition of deflections and rotations is allowed due to the fact that the stiffness of the structure is independent of x, y and φ if the linear theory utilised. The relatively large co-ordinates can be predicted by multiplication of the compliance matrix with the comb forces. The values of the other co-ordinates have been neglected. In the matrix equation below this is indicated with ≈0.

$$\begin{bmatrix} x1 \\ x2 \\ x3 \\ x4 \\ xm \\ ym \\ \varphi 1 \\ \varphi 2 \\ \varphi 3 \\ \varphi 4 \end{bmatrix} = \begin{bmatrix} c_x & \approx 0 & -c_x & \approx 0 \\ \approx 0 & c_x & \approx 0 & -c_x \\ -c_x & \approx 0 & c_x & \approx 0 \\ \approx 0 & -c_x & \approx 0 & c_x \\ c_x & \approx 0 & -c_x & \approx 0 \\ \approx 0 & c_x & \approx 0 & -c_x \\ \approx 0 & -c_\varphi & \approx 0 & c_\varphi \\ c_\varphi & \approx 0 & -c_\varphi & \approx 0 \\ \approx 0 & c_\varphi & \approx 0 & -c_\varphi \\ -c_\varphi & \approx 0 & c_\varphi & \approx 0 \end{bmatrix} \cdot \begin{bmatrix} F_{x1} \\ F_{x2} \\ F_{x3} \\ F_{x4} \end{bmatrix} \qquad [10]$$

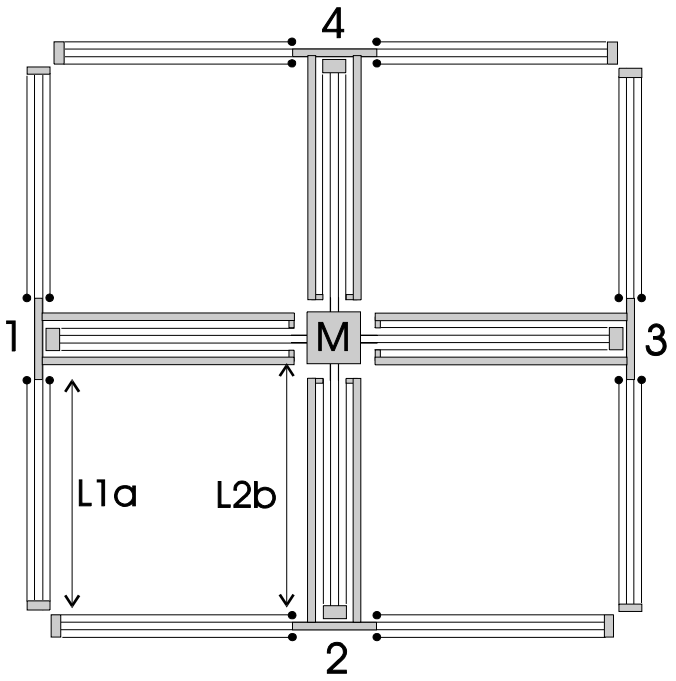

Fig.6: Xy-stage 2 is constructed with spring 7. The beams are fixed to the substrate at points indicated by the small dots.

with:

$$c_x = L_{1a}^3\beta_4 \Big/ L_{1a}^3 + 32Ebh^3\beta_4$$

$$c_\varphi = L_{1a}^3\beta_3 \Big/ L_{1a}^3 + 32Ebh^3\beta_4$$

$$\beta_1 = L_{1a}^3 \Big/ 16EI(L_{1a}^2 + 3L_{1a}L_c + 3L_c^2)$$

$$\beta_2 = \frac{4EI\beta_1(L_{1b} + h_c + L_m) + L_{1b}^2}{16EI\beta_1 + 8L_{1a}}$$

$$\beta_3 = \frac{\beta_1(L_{1b} + h_c + L_m) - 4\beta_1\beta_2}{4}$$

$$\beta_4 = \frac{24EI\beta_3(L_{1b} + h_c + L_m) + L_{1b}^3 - 6\beta_2 L_{1b}^2}{48EI}$$

Xy-stage 2: To avoid axial stresses still exhibited in xy-stage 1, a second design is proposed which is based on the seventh spring design (fig.6). It is expected to behave in the following manner:

1) Rotation of the moving electrodes is avoided because they are suspended by spring 7 which suppresses rotation. As a result, solely one spring has to be used to connect every moving electrode with the middle mass.
2) Compared to xy-stage 1, this design is suitable for large deflections because there are no axial stresses present in the individual springs.
3) The translational DOFs are very well uncoupled. For instance if comb 1 is activated, comb 2 and 4 will not move inwards due to lack of axial stresses as previously stated.

The spring constant in the desired direction of motion is derived following the same procedure previously described for the first xy-stage. It is concluded that the translational DOFs are uncoupled and secondly that comb rotations are zero. For this reason, the relationship between the actuator force and relevant co-ordinates is less complex. In this matrix, the compliance $c=1/k=L_{1a}^3L_{2b}^3/16Ebh^3(L_{1a}^3+2L_{2b}^3)$ is found by the summation of the stiffness' of the three flexures (1, 3, and middle).

$$\begin{bmatrix} x1 \\ x2 \\ x3 \\ x4 \\ xm \\ ym \end{bmatrix} = c \begin{bmatrix} 1 & 0 & -1 & 0 \\ 0 & 1 & 0 & -1 \\ -1 & 0 & 1 & 0 \\ 0 & -1 & 0 & 1 \\ 1 & 0 & -1 & 0 \\ 0 & 1 & 0 & -1 \end{bmatrix} \cdot \begin{bmatrix} Fx1 \\ Fx2 \\ Fx3 \\ Fx4 \end{bmatrix} \qquad [11]$$

6. DYNAMIC MODELLING OF XY-STAGES

The fundamental frequencies of all configurations will be determined in this section. Furthermore, the Q-factor, response time and dissipated power are important properties. Methods to obtain rough estimates of those properties are given as well.

Xy-stage1: The fundamental frequency can be found by slightly modifying the equation of spring 2 for ω_{r2}. If k_{xm} is equal to $\alpha.k_{x2}$, $k_{x1,xy1}$ is equal to $(2+\alpha).k_{x2}$. Therefore, the numerator is multiplied with $(2+\alpha)$. It is assumed that the fundamental mode shape of the beam connecting mass M with comb 2 and 4 is equal to the mode shape of a clamped beam. Strictly speaking, this is not true. The reason is the fact that the boundary conditions of this beam are different from a clamped beam due to rotation of comb 2 and 4. It can be shown that for usual dimensions, rotation is very small even for large deflections. Consequently, the kinetic energy of the rotating combs is negligible as well. Simulations have shown that this assumption is rather accurate. Concluding:

$$\omega_{r,xy1} = \sqrt{16Ebh^3(2+\alpha) \Big/ (m_c + 13m_s/35)\,L^3} \qquad [12]$$

Note that m_c and m_s are equal to the summation of the masses of the following structures:

m_c: Comb 1 and 3, the beam connecting mass M with comb 1 and 3 and mass M itself.

m_s: The thin beams supporting comb 1 and 3 and the beam connecting the other combs with mass M.

Xy-stage2: Slight modification of the equation for ω_{r7}, gives the resonance frequency for xy-stage 2. It is found by multiplying the factor $2(n^2-2n+2)$ with $(2+\alpha)$.

Q-factor: The Q-factor is dependent on damping [5]. There are several damping mechanisms limiting the overall Q, where each damping mechanism can be related to a specific Q-factor; viscous and acoustic damping, Q_a, damping due to imbalances, Q_s, damping resulting from internal material related losses, Q_i, and damping due to losses related to external circuitry, Q_e [6]. These Q-factors can be related to

the total Q-factor as: 1/Q=1/Qa+1/Qs+1/Qi +1/Qe. This relationship indicates that it is the lowest Q-factor of the different mechanisms which limits the total Q. Applied to xy-stages made of single-crystalline silicon, intrinsic Q_i-factors are usually very high. Therefore, for xy-stages operated in ambient air, damping due to internal losses can be neglected. A vibrating surface creates a lateral, as well as a perpendicular movement of the gas surrounding the surface. The perpendicular movements results in radiation losses and will be neglected because the surfaces only moves laterally to the substrate. The lateral transport generates viscous energy losses and is estimated by assuming Couette flow underneath the resonating mass [7]. The total Q-factor of the device without external circuits, is given by:

$$Q \approx \frac{d_{offset}}{\mu A}\sqrt{M_t k_t} \qquad [13]$$

where μ is the absolute viscosity of the surrounding gas (for air $\mu=1.8.10^{-5}Nsm^{-2}$), A_t is the surface area of all resonating structures, d_{offset} is the offset between the vibrating structure and the substrate, M_t is the mass of the supporting beams, and k_t is the spring constant of the entire flexure structure in the direction of vibration. It should be stated that this equation only gives a rough estimate of the Q-factor. However, for design purposes this will be a useful approximation.

Response time: This property describes the time needed for the structure to approximate the displacement in steady state for a given constant comb-actuator force within 5%. The response time is directly related to the Q-factor. The mechanical response time can be estimated by [8], with f_o, the resonance frequency:

$$\tau_m = t_{5\%} = Q/f_0 \qquad [14]$$

Dissipated power: Power will be dissipated due to damping. The quality factor is defined as Q=2π (*vibration energy per cycle)/ (energy loss per cycle).* The vibration energy is equal to the maximum potential or maximum kinetic energy. The maximum potential energy is equal to $\Delta Vmax=½k_t x_{max}^2=E_{vib}$. After k_t has been determined for every xy-stage. The energy dissipation per second will be equal to f_0 times the energy loss per cycle [8]:

$$P_{dis} \approx 2\pi f_0 E_{vib} / Q \qquad [15]$$

7. FINITE ELEMENT ANALYSIS

A major part of the presented work is concerned with the modelling of rather extensive mechanical spring structures using the theory of linear elasticity. The finite element system COSMOS used for the simulation of the mechanical comb-structures is capable of performing simulations based on linear elasticity. Therefore, COSMOS is a powerful tool for the validation of the linear models of xy-stages. Because errors are inherent in any simulation, estimates on the simulation errors ought to be made. For this purpose test simulations on structures of which the linear models are readily available, such as a simple and clamped beam, should be done.

The following conclusions regarding the static behaviour of springs can be drawn:

1) The maximum difference between the theoretical and simulated spring rates is 2.6 % for the desired and 6.9 % for the undesired direction of motion respectively.
2) The spring rates of spring 2, 3 and 4 are all smaller than the theoretical values. This can be explained by the fact that the thick beam sections are not completely rigid.
3) The effect mentioned in conclusion 2, is more pronounced for loads in the y-direction. This is caused by the fact that k_y is proportional to h/L and k_x to h^3/L^3. As a result, the selectivity will be decreased for longer thick beams.
4) Whether spring 2 and 4 are subjected to a pressure or a force in the x-direction does not significantly alter the deflection. This can be explained by the fact that the thick beam sections are very rigid compared to the thin beam sections in the x-direction.
5) The difference between theory and simulations is to a large extend caused by the assumptions made and not due to simulation errors. Especially the assumption that the thick beam sections are completely rigid has a significant influence. For instance, if the elasticity of the thick beam section of spring 2 is taken into account, the error in k_y is reduced from 5.6 % to 0.9 %.

The following conclusions regarding the dynamic behaviour of springs can be drawn:

1) The maximum difference between the theoretical and simulated fundamental frequencies is 6.9 %.
2) The theoretical resonance frequencies are all larger than the simulated resonance frequency. This is in agreement with the fact that assuming any mode shape except the actual one, results in an ω_r larger than the actual ω_r.
3) The dynamic mode shape is not equal to the static deflection. A better estimation of the dynamic mode shape can be obtained by using the Raleigh-Ritz method.
4) The theoretical value of spring 2 is more accurate compared to spring 1. This is due to the fact that the mode shape of the thick beam section can be estimated more accurately compared to the thin beam sections. As expected, the errors for spring 1 and 3 are almost identical. This is due to the fact that both flexures mainly consist of thin beams.
5) For yet unknown reasons, the discrepancy between theory and simulation is relatively large for spring 4.
6) It is likely that the difference between theory and simulations is mainly caused by the assumption of a suitable mode shape and not due to simulation errors.

The following conclusions regarding the static behaviour of xy-stages can be drawn:

1) The maximum difference between the theoretical and simulated spring rates is 4.3 % for the desired and 7.3 % for the undesired direction of motion respectively. As previously concluded for individual springs, this is due to the neglect of the elasticity of the thick beam sections.
2) The maximum difference between the theoretical and simulated rotations of xy-stage 1 is 5.4 %.
3) Simulations have confirmed that co-ordinates which were assumed to be small can be neglected.
4) Rotation of the combs of xy-stage 2 is only 10 % of the rotation of xy-stage 1. Therefore, it can be concluded that undesired rotation is effectively reduced.

The following conclusions regarding the dynamic behaviour of xy-stages can be drawn:

1) The maximum difference between the theoretical and simulated fundamental frequencies is 5.6 %.
2) The theoretical resonance frequencies are all larger than the simulated resonance frequency. This is in agreement with the fact that assuming any mode shape except the actual one, results in an ω_r larger than the actual ω_r.
3) Momentary it is unknown in which direction xy-stage 2 prefers to vibrate. Simulations indicate that the vibration direction is in the direction exactly in between the two DOFs, x and y.
4) As already concluded for individual springs, it is likely that the difference between theory and simulations is mainly caused by the assumption of a suitable mode shape and not due to simulation errors.

8. MODELLING OF ELECTROSTATIC COMBS

This chapter investigates the electrostatic drive and sense, using an interdigitated capacitor (electrostatic comb). Fig.7 schematically represents an electrostatic comb. The following parts can be distinguished: fixed electrodes, movable electrode, comb fingers, flexure, and a power source or capacitance-meter, connected with the fixed electrodes, depending on the operation mode. The electrodes form two capacitance's which are used in a series connection. The flexures are used to prevent the moving electrode from moving in the undesired direction of motion. One of the advantages of this actuator type is the independence of the actuator force of the displacement. It is desirable to use low driving voltage and therefore ways of reducing the drive voltage are summarised. Electrostatic combs can also be used as a position sensing device. A deflection of the mechanical springs brings on a capacitance change per unit displacement which is independent of the displacement. In other words, the relationship between displacement and capacitance is linear which is very convenient when measuring the displacement using a capacitance-meter. With increasing drive voltage, the comb actuator is more likely to become unstable. The actuator stops operating as a result of the short-circuit. Large mechanical spring rates in the undesired direction of motion prevents the comb fingers from sticking to each other.

Electrostatic comb-drive: To be able to move the suspensions, electrostatic combs are used in the actuation mode. In this situation, an external voltage source is connected to the fixed electrodes.

The following notations have been used in the next discussion: n=number of comb fingers per fixed electrode (n=3), l=length of comb finger, x=displacement of free electrode in the stroke direction, d=gap width, b=structure width, F_X=actuator force in the stroke direction

The moving electrode is used to form two comb capacitance's which are used in a series connection. The advantage of this actuation principle is the fact that the potential of the moving electrode is left floating. Both capacitors have the following value:

$$C = \varepsilon_0 \varepsilon_r A/d = \varepsilon_0 \varepsilon_r (2n-1) xb/d \qquad [16]$$

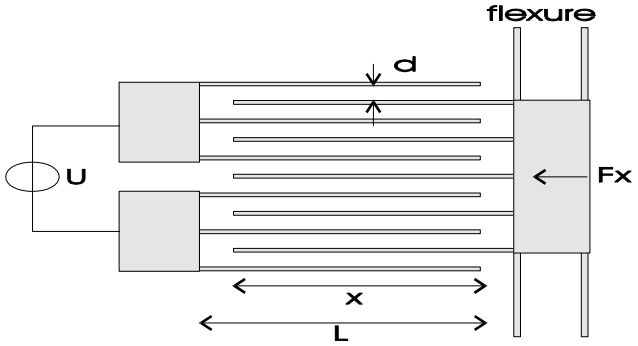

Fig.7: Comb-actuator(/sensor).

Because of the series connection of the capacitors, the resulting capacitance, C_t will be half this value and the energy stored is equal to:

$$E = C_t U^2 / 2 = \varepsilon_0 \varepsilon_r (2n-1) xbU^2 / 4d \qquad [17]$$

The comb force in the stroke direction, F_X, is per definition equal to the partial derivative of the energy function to the position x:

$$F_x = \partial E / \partial x = \varepsilon_0 \varepsilon_r (2n-1) bU^2 / 4d \qquad [18]$$

It can be seen that the maximum comb force is limited by the maximum operating voltage U_{max}.

The comb force causes a deflection of the spring. It is desirable to reach a certain displacement with a driving voltage as low as possible. Low driving voltages can be obtained by varying the following variables:

1) The actuator force is proportional to the number of comb fingers. The number of fingers can be increased in two ways. First of all, more fingers can be placed in a row. Secondly, it is possible to place a number of rows behind each other [9]. The disadvantage of increasing n, is the simultaneous increase of the device area.
2) The actuator force is proportional to the structure width. Increasing the structure width however is not enough to reach a larger deflection because the spring constant of the mechanical structure is also proportional to b. Therefore it can be concluded that increasing the structure width is only effective when the width of the spring structure is not increased simultaneously.
3) Decreasing the gap between the fingers will also increase the actuator force because F_X is inversely proportional to d. The disadvantages of this method are the following. First of all it should be mentioned that the processing techniques to reach smaller gaps will be more complex. Secondly, the actuator stability decreases for smaller gaps.
4) A more theoretical way to increase the actuator force is to use another medium in between the comb fingers. It is possible to encapsulate a liquid with a large dielectric constant. A disadvantage of this method is the fact that the Q-factor of a comb-drive used in a resonating configuration will be decreased drastically. For applications in which the only design consideration is a large actuator force and low damping is of minor importance, using a different medium could be a useful option.

Maximising the actuator force is not the only important issue. It is also important that the device dimensions should not be increased too drastically which will be the case if the number of comb fingers is very large. Therefore, the ratio L_c/L has to be optimised to reach a maximum deflection for a certain constant spring length, L_{tot}, which is equal to L_c+L. By looking at the extreme values of L_c/L, 0 and ∞ respectively, it can be seen that an optimum exists in between the two extremes. In situations where $L_c/L=0$, the actuator force is zero. If $L_c/L=\infty$, in other words when L=0, the spring constant is infinite. For both situations, the spring is not deflected. The next step is to find the best ratio. The spring deflection is equal to F_x/k_x. It can be seen that F_x is proportional L_c and k_x to L^{-3}. Furthermore, $L_c=L_{tot}-L$. In other words, x can be expressed as follows:

$$x = const.(L_{tot} - L)L^3 \qquad [19]$$

The optimum is found by differentiation of x with respect to L and equating to zero. This predicts a best ratio of L_c/L is 1/3.

Electrostatic comb-sense: Due to a displacement of the movable electrode relative to the fixed electrode, the capacitance between the fixed electrodes will alter. As a result it can be concluded that the capacitance is a measure for the position of the movable electrode. The capacitance change per unit displacement is constant and is given by the partial derivative of the capacitance to the displacement:

$$\partial C_t / \partial x = \varepsilon_0 \varepsilon_r (2n-1)b/2d \qquad [20]$$

In other words, the relationship between capacitance and displacement is linear. This property of electrostatic combs is very convenient for displacement measurements.

Stability analysis: Here, "unstable" means the situation in which the fingers of the moving electrode move in the direction perpendicular to the stroke direction and touch the stationary electrode. In this case, a short-circuit between the stationary and moving electrode occurs and the actuator stops operating.

Three causes for instability can be distinguished. The first reason for the fingers to interconnect could be the result of external forces and moments on the structure to which the comb fingers are attached. Examples of external loads are forces originating from the macro world and forces c.q. moments due to other comb-drives. The next two reasons are due to the electrostatic attraction between the comb fingers in the direction perpendicular to the stroke if the fingers are out of centre. The tip of the fingers deflect in the y-direction. This is especially the case for long thin fingers because of their higher flexibility and larger capacitance area. If the fingers are assumed to be completely rigid, the movable electrode also tends to move in the direction perpendicular to the stroke. In the next discussion, the latter effect is modelled and the effect of reducing the interelectrode gap is discussed.

The following notations have been used in the discussion below: U=applied voltage, x=displacement of free electrode in the stroke direction, y=displacement of free electrode perpendicular to the stroke, d=gap width, b=structure width, F_y=actuator force perpendicular to the stroke direction, k_x=spring constant in the stroke direction, k_y=spring constant perpendicular to the stroke

With increasing drive voltage, the comb actuator is more likely to become unstable. The electrostatic force F_y is generated by the fact that the moving electrode moves a distance y in the y-direction. Note that y=0 when the moving finger is positioned precisely at the centre of the gap. F_y generated by both sides of the parallel plate per moving finger, is:

$$F_y = \frac{1}{2}\varepsilon_0 \varepsilon_r bxU^2((d-y)^{-2} - (d+y)^{-2}) \qquad [21]$$

A positive value of F_y proves that the suspended electrode is unstable [10]. It looks as if there were a negative spring. The equivalent "negative" spring constant k_e when the moving finger is placed at the centre of the gap is:

$$k_e = \left.\frac{\partial F_y}{\partial y}\right|_{y=0} = 2\varepsilon_0 \varepsilon_r bxU^2/d^3 \qquad [22]$$

The mechanical spring with spring constant k_y keeps the moving finger in a stable position as long as its absolute value is larger then the absolute value of k_e. Therefore the minimum value of k_y is:

$$|k_y| > |2\varepsilon_0 \varepsilon_r bxU^2/d^3| \qquad [23]$$

Both terms can be controlled independently. Note that in situations where the number of moving fingers is more than one, k_y has to be larger. The most effective way to decrease this type of instability is to increase the selectivity k_y/k_x. This is one of the reasons why so much effort has been made to optimise the spring design. To minimise the driving voltage needed to reach a certain deflection, k_x has to be as low as possible. Another important design consideration is to minimise the initial overlap length of the comb fingers.

9. EXPERIMENTAL & CONCLUSIONS

Several xy-stages have been fabricated with the help of the black silicon method (BSM) [11-13]. Axial stress which is responsible for non-linear behaviour is avoided due to a folded beam structure, the electrical connection is split to avoid deflection of the stage in the Z-plane, the beam- to comb-width ratio is optimised, the construction is such that the x- and y-direction are minimally coupled and extra beams are used to avoid the rotation of a comb and thus preventing short circuit. Measurements on both stages, with typical dimensions of 1mm square, have been performed and it is found that xy-stage 1 has a deflection of only a few microns for several hundreds of volts. Xy-stage 2 is much easier to deflect: 15 volts is enough to deflect the stage 25 microns in one direction. The measured deflection are in excellent agreement with the theory. This performance is increased when operating the structures in (dielectric) liquids such as isopropanol, demiwater, or fluorinert®. Although now only a few volts are needed for maximum deflection, caution must be taken to prevent bubble generation because of electrolyses. At the same time, it is found that the dynamic behaviour is changed dramatically. At frequencies exceeding 10 Hz

complex vibration phenomena are observed. In contrast, the stages operating in open air have resonance frequencies between one- and one hundred kHz as predicted by theory. In total, it can be concluded that theory, simulation and experiments are in excellent agreement and for that reason it is possible to design micro-mechanical structures while using simple mathematical algorithms.

10. REFERENCES

[1] J.M.Gere, S.P.Timoshenko, *Mechanics of materials,* PWS Engineering, Boston, Massachusetts, 1987

[2] H.V.Jansen, *Thermische actuatie van een micropomp*, internal report, University of Twente, 1991

[3] G.J.M.Gouverneur, *The study of the static deflection of a double fixed-end spring (beam); the non-linear theory,* internal report, University of Twente.

[4] R.F.Steidel, Jr., *An introduction to mechanical vibrations,* John Wilet & Sons, Inc., 1989

[5] G.Stemme, *Resonant silicon sensors,* J.Micromech. Microeng.1(1990)

[6] A.Prak, *Silicon resonant sensors: operation and response,* PhD thesis, University of Twente, 1993.

[7] W.C.Tang, T.C.H.Nguyen, R.T.Howe, *Laterally driven polysilicon resonant microstructures,* Sensors and actuators, 20 (1989).

[8] H.V.Jansen, *Een micromechanische laserstraal afbuiger,* TNO report, University of Twente, 1991.

[9] V.P.Jaecklin, C.Linder, F.de Rooij, J.M.Moret, R.Bischof, F.Rudolf, *Polysilicon comb actuators for xy-stages,* Micro Electro Mechanical Systems '92, Travemunde, 1992.

[10] T.Hirano, T.Huruhata, K.J.Gabriel, H.Fujita, *Design, fabrication, and operation of submicron gap comb-drive microactuators,* J.of Micro Electro Mechanical Systems, Vol.1, No.1, 1992.

[11] H.Jansen et al, EP appl.No.94202519.8.

[12] H.Jansen et al, *The Black Silicon Method:...*, Proc. Micro Mechanics Europe (MME'94, Pisa, Italy), Sep. 1994, p.60-64.

[13] H.Jansen et al, *The Black Silicon method II:...*, Proc. Micro and Nano Engineering (Davos, Switzerland), Sep. 1994, p.312-313.